Supplement of Atmos. Chem. Phys., 22, 823–845, 2022
https://doi.org/10.5194/acp-22-823-2022-supplement

Atmospheric Chemistry and Physics
Open Access
EGU

Supplement of

Box model trajectory studies of contrail formation using a particle-based cloud microphysics scheme

Andreas Bier et al.

Correspondence to: Andreas Bier (andreas.bier@dlr.de)

Derivation of an average trajectory from a trajectory ensemble

We define the relative expansion factor $f_{X,Y}$ in terms of attribute *Y* for a trajectory set *X*.

$$f_{X,Y} := \frac{Y_X}{Y_{X,0}} \quad \text{(S1)}$$

Hereby, *X* can be an average trajectory *AT*, a trajectory ensemble *EM* or a single trajectory of the ensemble *i*. The subscript "0" stands for the initial state at the engine exit. The attribute *Y* can be the temperature *T*, the excess temperature $\Delta T = T - T_a$, cross-section *A* or mass *M* of the trajectory set *X*, where T_a is the ambient temperature.

For the definition of the average trajectory we require that

$$f_{AT,Y} = f_{EM,Y} \quad \text{(S2)}$$

(i.e., the relative expansion factor of the average trajectory matches that of the trajectory ensemble). The relative expansion factor of the trajectory ensemble is defined as

$$f_{EM,Y} := \overline{f_{\iota,Y}} \quad \text{(S3)},$$

where the overbar denotes averaging or summation over all trajectories *i* (depending on whether *Y* is an intensive or extensive quantity).

For now, we leave it open, which weighting attribute *Y* is the most suitable.

The relative expansion factors behave as follows (S4c results from Eq. 16 in the main manuscript):

$$f_{X,T} = \frac{T_X}{T_{X,0}} \quad \text{(S4a)}$$

$$f_{X,\Delta T} = \frac{\Delta T_X}{\Delta T_{X,0}} \quad \text{(S4b)}$$

$$f_{X,M} = \frac{M_X}{M_{X,0}} = \mathcal{D}_x^{-1} = f_{X,\Delta T}^{-1} \quad \text{(S4c)}$$

$$f_{X,A} = \frac{A_X}{A_{X,0}} = \frac{T_X}{T_{X,0}} \mathcal{D}_x^{-1} = f_{X,T}\, f_{X,\Delta T}^{-1} \quad \text{(S4d)}$$

Plugging S4c and S3 into S2, we obtain a relation for T_{AT}

$$\mathcal{D}_{AT}^{-1} = \frac{1}{N}\sum_{i=1}^{N} \mathcal{D}_i^{-1} \Rightarrow \Delta T_{AT}^{-1} = \frac{1}{N}\sum_{i=1}^{N} \Delta T_i^{-1} \quad \text{(S5)}$$

Analogously we can use S4a or S4b to obtain (in both cases identical) definitions of T_{AT}

$$T_{AT} = \frac{1}{N}\sum_{i=1}^{N} T_i \Leftrightarrow \Delta T_{AT} = \frac{1}{N}\sum_{i=1}^{N} \Delta T_i \quad \text{(S6)}$$

Note that Eqs. S5 and S6 give two differing definitions of T_{AT}. In the main manuscript, we use Eq. S6 to define the average trajectory. Yet, the definition S5 has the favourable property that the mass of the average trajectory is identical to the sum of the masses of the individual trajectories.

Ensemble properties

Ensemble properties can be defined by the following procedure: A ensemble property Z_{EM} is obtained by averaging the quantity *Z* over the ensemble and requiring the following to hold:

$$f_{EM,Y} * Z_{EM} := \overline{f_{\iota,Y} * Z_\iota} \Rightarrow Z_{EM} = \overline{f_{\iota,Y} * Z_\iota} / \overline{f_{\iota,Y}} \quad \text{(S7)}$$

Throughout the main manuscript we use a mass-weighted averaging (i.e. $Y = M$).

$$Z_{EM} = \overline{M_i * Z_i}/M_{tot} \qquad \text{(S8)}$$

Box model results for two types of averaging

In the main manuscript the unweighted temperature average according to Eq. S6 was used to derive the temperature of the average trajectory. Consistent with the mass-weighted averaging (Eq. S8), the mass-conserving computation of the average temperature (according to Eq. S5) would have been the more appropriate choice. In the following, we compare average traj simulation results for both types of T_{AT}-definitions (Eqs. S5 and S6).

Figure S1 left shows that the mass-conserving T_{AT} (red) decreases faster than the original unweighted temperature average (blue).

In the following, we aim at investigating the impact of the different trajectory averaging methods on the results of selected box model simulations. Figure S2 shows the quantities analogously to our Fig. 2 in the main manuscript. Since plume cooling proceeds faster, the first exceedance of plume water saturation and the peak relative humidity is reached earlier (by around 0.05 s at T_a = 220 K and 0.15 s at T_a = 225 K) for the mass-conserving than for the unweighted average traj (Fig. S2 a,b). This causes (consistent with the time offset in relative humidity) an earlier droplet formation on soot particles (Fig. S2 c,d). Since droplet growth proceeds faster due to an initially stronger increase in plume relative humidity, there is less time do deplete water vapor due to condensation loss on the larger soot particles. Hence, some smaller soot particles manage to overcome the Köhler barrier and to activate into water droplets and the activation fraction (dashed lines in Fig. S2 c,d) for the mass-conserving average traj is slightly higher than for the unweighted average traj. Since nearly all droplets freeze to ice crystals, the freezing fraction of soot particles (solid lines) is larger for the mass-conserving average traj (0.93 instead of 0.89 at T_a = 220 K and 0.42 instead of 0.39 at T_a = 225 K) as well.

In a next step, we investigate how the freezing fraction of soot particles $\varphi_{frz,f}$ (shown in Fig. S1 right) depends on ambient temperature. As already displayed in Fig. 5c of the main manuscript, $\varphi_{frz,f}$ typically increases with decreasing T_a or, equivalently, increasing ΔT (temperature difference between T_a and Schmidt-Appleman threshold temperature). For the mass-conserving average traj (red), the temperature dependency of the final freezing fraction lies well in between that for the unweighted average traj (blue) and the ensemble mean (magenta). Hence, we find a smaller discrepancy between the ensemble mean and the average trajectory, when we employ the mass-conserving averaging method.

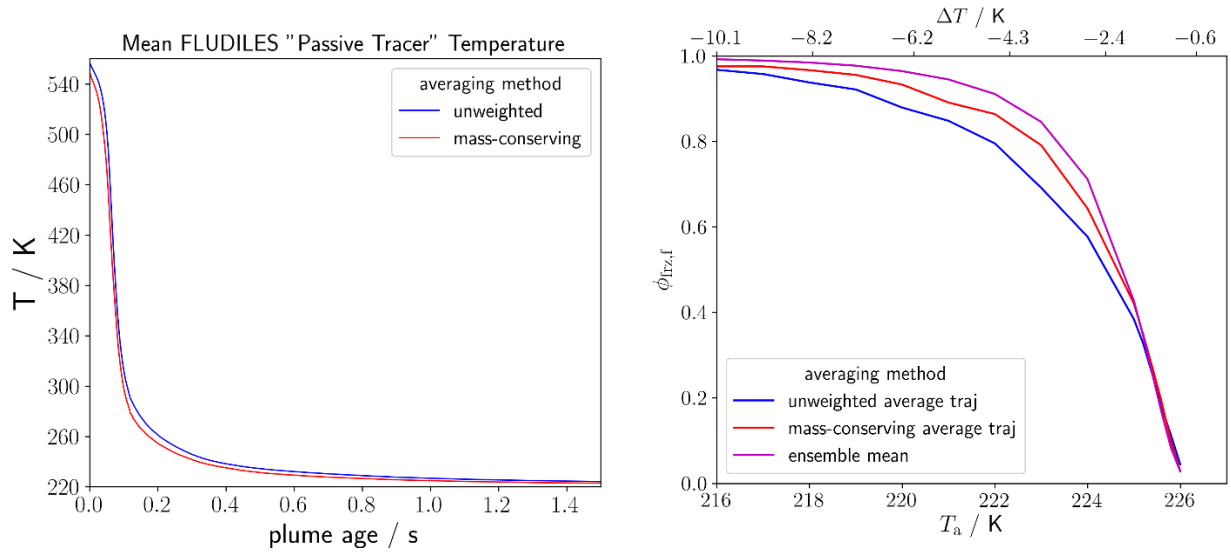

Figure S1. Left: Temporal evolution of FLUDILES "passive tracer" temperature averaged over the 25000 trajectories using an unweighted (blue) and a mass-conserving average (red); right: fraction of soot particles freezing to ice crystals $\varphi_{frz,f\,s}$ at a plume age of 2 s depending on ambient temperature T_a (where the axis on the top additionally shows the temperature difference to the Schmidt-Appleman threshold temperature) for the average traj with both averaging methods from the left panel and for the ensemble mean evolution (magenta). For the right panel, we use the baseline parameters from Table 1 of the main manuscript.

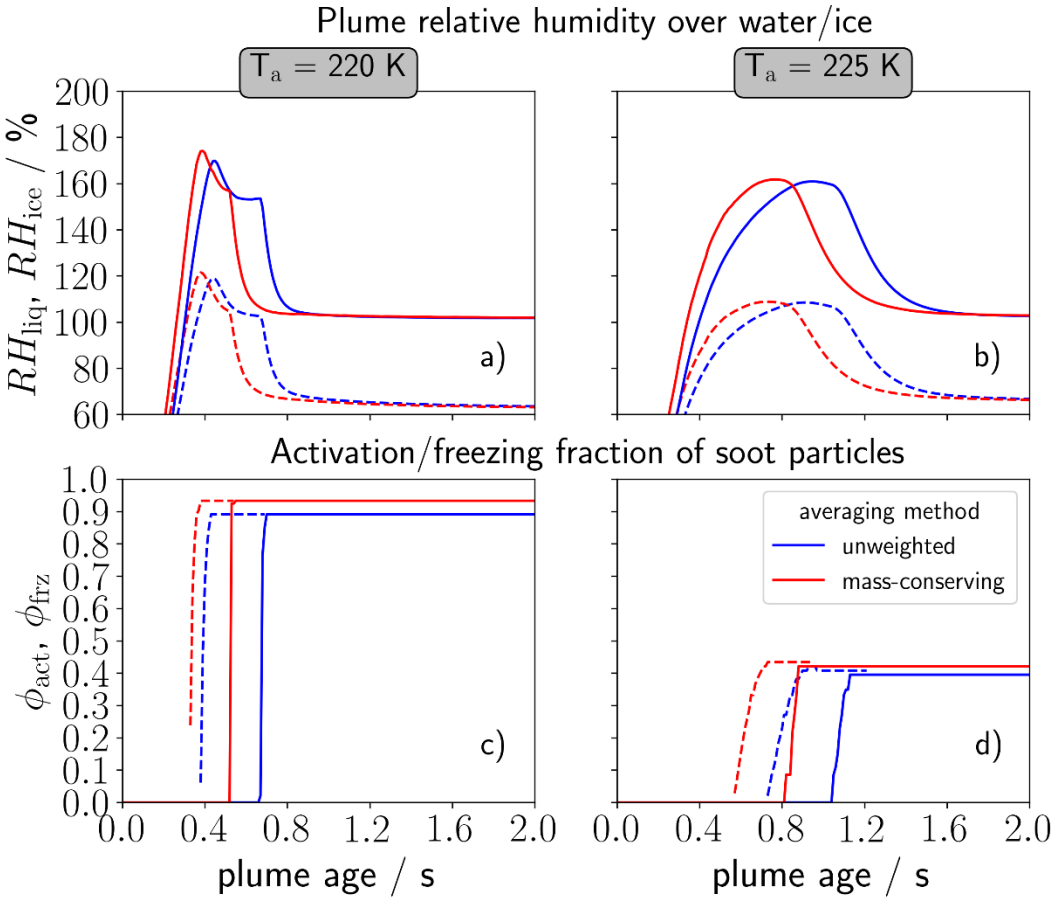

Figure S2. Temporal evolution of (top row) plume relative humidity over water (dashed) and ice (solid) and of (bottom row) fraction of soot particles activating into water droplets (dashed) and forming ice crystals (solid). The left column shows the baseline case with ambient temperature T_a = 220 K, the right column the near-threshold case with T_a = 225 K. We show the results for the unweighted (blue) and the mass-conserving average trajectory evolution (red).